Manufacturing Rev. 2014, **1**, 4

DOI: 10.1051/mfreview/2014003

Manufacturing Review

Available online at:
http://mfr.edp-open.org

RESEARCH ARTICLE OPEN ACCESS

Punching process including thickening of hole edge for improvement of fatigue strength of ultra-high strength steel sheet

Purwo Kadarno*, Ken-Ichiro Mori, Yohei Abe, and Tatsuro Abe

Department of Mechanical Engineering, Toyohashi University of Technology, Toyohashi, Aichi 441-8580, Japan

Received 19 February 2014 / Accepted 22 March 2014 / Published online 5 May 2014

Abstract – A punching process including thickening of a hole edge of an ultra-high strength steel sheet with a taper punch and step die was developed to improve fatigue strength of the punched sheet. In this process, the sheet was punched by the bottom of the punch, and subsequently the hole edge was thickened by the taper of the punch and the corner step of the die. The taper angle of the punch and the step height of the die were optimised to increase the amount of thickening. The quality of the sheared edge for the thickened punched sheet was improved by ironing with the taper of the punch, and compressive residual stress was generated around the hole edge. Seizure on the surface of the punch was prevented by VC-coating for repeated punching and realistic punching speed. It was found that the present punching process including thickening is effective in improving the fatigue strength of the punched ultra-high strength steel sheet and in preventing occurrence of delayed fracture.

Key words: Punching, Thickening, Hole edge, Ultra-high strength steel sheet, Fatigue strength

1 Introduction

To improve the fuel efficiency of automobiles, the reduction in weight of body panels has become a high priority for a vehicle development. Kleiner et al. [1] have reviewed technologies of metal forming processes of lightweight components for the reduction. Among lightweight materials, high strength steel sheets are the most attractive material for body-in-white parts due to the high specific strength and cost competitiveness. In stamping operations of high strength steel sheets, large springback, small formability, short tool life, etc. are problematic, particularly for ultra-high strength steel sheets having a tensile strength above 1 GPa. Mori et al. [2] have decreased springback in bending of ultra-high strength steel sheets by a small additional reduction in thickness at the bottom dead weight centre.

Body-in-white parts are generally punched to make many holes for joining, paint removing, attachment, reduction in weight, etc. In punching of high strength steel sheets, tools tend to wear and chip due to large punching load, and thus the tool life is short. Eriksson and Olsson [3] have improved the tool life in stamping of high strength steel sheets by the PVD coatings. Inoue et al. [4] have observed damage of VC and TiC coated tools in stamping of ultra-high strength steel sheets. In addition, the quality of the sheared edge deteriorates due to early onset of cracks for the small ductility, the increase in rough fracture surface.

In high strength steel sheets, the static strength of formed products is almost proportional with the strength of the sheet, whereas Murakami et al. [5] have reported that the increase in the fatigue strength becomes gradually small. Thomas et al. [6] have observed that onset and progress of fatigue cracks of punched high strength steel sheets are accelerated around holes due to concentration of stress, particularly for rough fracture surface and sharp burr of the sheared edge. Therefore, the improvement of the quality of the sheared edge of punched sheets is useful for increasing the fatigue life. Thipprakmas et al. [7] have improved the quality of the punched edge of aluminium sheets by shaving with a taper punch. Kim et al. [8] have developed a burr-free punching process consisting of mechanical half piercing and hydro counter punching. Mori et al. [9] have smoothed the fracture surface of the sheared edge using the conical punch to improve the hole expansion ratio of the punched ultra-high strength steel sheet. Mori et al. [10] have improved a sheared edge of ultra-high strength steel sheets in slight clearance punching with a punch having a small round edge. Abe et al. [11] have developed a gradually contacting punch for improving stretch flangeability of ultra-high strength steel sheets. Mori et al. [12] have developed a warm and hot

*e-mail: kadarno@plast.me.tut.ac.jp; pkadarno@gmail.com

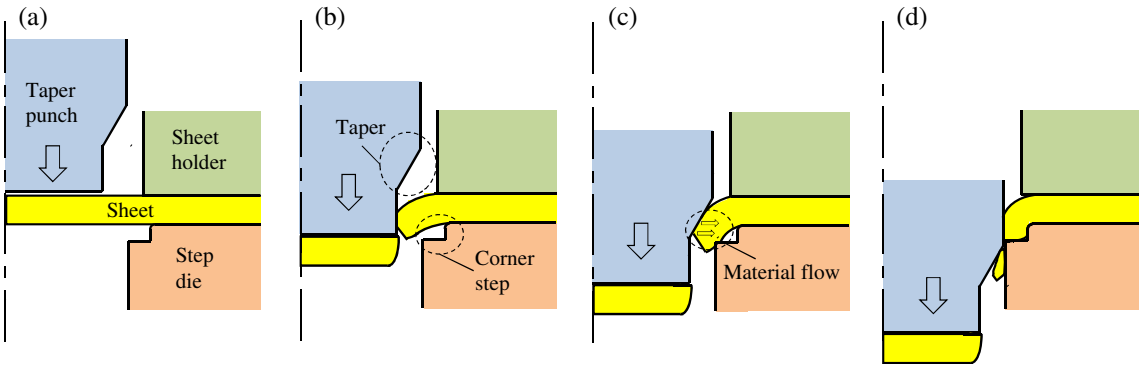

Figure 1. Punching process including thickening of hole edge for increasing fatigue life of ultra-high strength steel sheet. (a) Initial, (b) punching, (c) thickening and (d) cropping stage.

punching process using resistance heating to improve the quality of sheared edge of the ultra-high strength steel sheet. Thomas [13] has examined the effect of the clearance ratio on the quality of the sheared edge, the formability and the fatigue life of the punched sheets in punching of high strength steel sheets. Matsuno et al. [14] have employed a punch having a round corner and an inclined bottom for punching of thick high strength steel sheets and examined the fatigue properties of the punched sheets. Although the fatigue strength is improved by the quality of the sheared edge, the improvement is not enough to extend the applicable range of ultra-high strength steel sheets.

The concentration of stress around the punched hole is relieved by increasing the thickness around the hole edge, and thus the fatigue strength may be improved. Nakano [15] has reviewed plate forging processes including local thickening. Merklein et al. [16] have reviewed sheet-bulk metal forming processes for controlling wall thickness of formed products. Although incremental forming processes such as flow forming, shear spinning and orbital forming have high ability in controlling metal flow due to repeated local deformation, the productivity is not high. It is desirable in industry to develop a stamping process having high productivity. Kadarno et al. [17] have examined the effect of the thickening of the hole edge by flanging on the fatigue strength of punched high strength steel sheets. Thipprakmas et al. [18] have examined the effect of the quality of the sheared edge of the initial hole on the flanged shape in hole flanging. Since the hole flanging stage is added to the punching process, the number of stages increases by one.

In the present study, a punching process including thickening of a hole edge of ultra-high strength steel sheets was developed to improve fatigue strength of the punched sheets. Shapes of a punch and die were design for succession of punching and thickening stages. The effect of the thickening on the strength of the punched sheets was evaluated from the experiment.

2 Punching process including thickening of hole edge

To improve the fatigue strength of punched ultra-high strength steel sheets, an edge of the punched hole was thickened. A hole flanging operation is conventionally performed

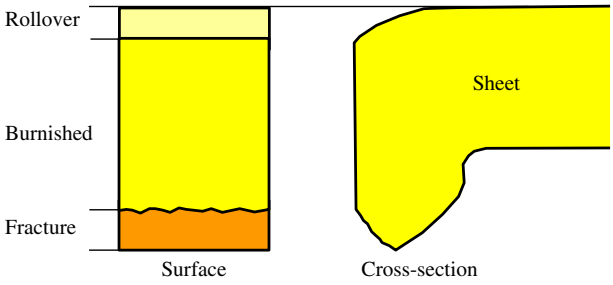

Figure 2. Surface and cross-section of thickened hole edge without compression of sharp bottom for excessive height of corner step.

subsequently to a punching operation, and thus the number of stages increases by one. In the present study, a pair of taper punch and step die was designed to include thickening of the hole edge in the punching process through one shot as shown in Figure 1. The sheet is first punched by the tension between the taper punch and the step die. Subsequently, the hole edge is bent by the taper of the punch into the corner step of the die and the surface of the sheared edge is ironed. After sufficient filling into the corner step of the die, the excessive material is then sheared. The corner step of the die has the function of not only forming the thickened edge but also compressing the edge bottom. The function is effective for ultra-high strength steels sheets having low ductility. Although the firstly punched hole is smaller than the desired hole, the hole is formed into the desired one by the subsequent thickening stage. A part of the punching scrap is effectively utilised as thickening material in the present process. This is an ecological process for improving material efficiency. In addition, it is easy to install the present punching process in the stamping sequence.

The amount of thickening of the hole edge in the present punching process is influenced by the shapes of the punch and die. As the diameter of the punch bottom decreases, the material for forming the thickened edge increases due the decrease in diameter of the punched hole, and thus the amount of thickening becomes large. Although this material is filled into the corner step of the die, the sharp edge bottom having remaining fracture surface is not compressed for excessive height and width of the corner step as shown in Figure 2. This leads to onset of fatigue cracks.

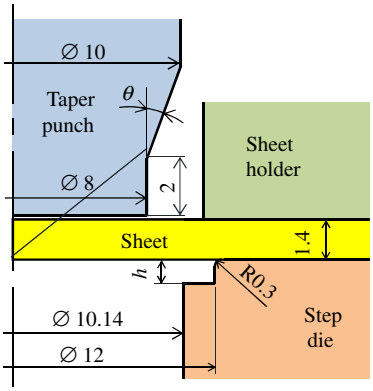

Figure 3. Dimensions of tools used in punching process including thickening of hole edge of ultra-high strength steel sheet.

Table 1. Conditions of punching process of ultra- high strength steel sheet.

Taper angle of punch θ	10°, 13° and 20°
Step height of die h	0.5, 0.7, 0.9 and 1.1 mm
Punch	SKD11, VC coating
Die	SKD11, no coating
Punching speed	0.08 mm/s
Lubrication	Rust prevention oil

In the present study, the diameter of the punched hole was set to be 10 mm typical of body-in-white parts. The dimensions of the tools are shown in Figure 3. The diameter of the punch bottom was smaller than that of the desired hole to thicken the hole edge. For a diameter of the punch bottom of 8 mm, the theoretical amount of thickening for complete filling without cropping loss is 1.1 mm. The amount of thickening was adjusted by the step height of the die h and the taper angle of the punch θ under fixing the step diameter at 12 mm.

The conditions of the punching process including thickening of the hole edge of an ultra-high strength steel sheet are given in Table 1. The sheets were punched by a 50 kN screw driven type universal testing instrument. A rust prevention oil was applied to the sheets and an additional lubricant was not employed. Each punching test was performed at least two times.

The ultra-high strength steel sheet JSC980 having a nominal tensile strength of 980 MPa and was used in the experiment, where the high strength steel sheet JSC590 was punched as a comparison. The 980 MPa sheets having 1.4 mm in thickness are the commonest ultra-high strength steel sheets and application to automobile body panels is recently increasing. The mechanical properties and the flow stress curves of these sheets measured from the tensile test are given in Table 2 and Figure 4, respectively. The specimens were cut in the 0°, 45° and 90° directions with respect to the rolling direction of the sheets, and the averages of the measured values are shown.

Finite element simulation using the commercial software ABAQUS was performed under the assumption of axi-symmetric deformation to examine deformation behaviour during the punching operation. The sheet was modelled to be

Table 2. Mechanical properties of ultra-high strength steel sheet.

	JSC980	JSC590
Thickness	1.4 mm	
Flow stress curves	$\sigma = 1574\varepsilon^{0.14}$ MPa	$\sigma = 979\varepsilon^{0.16}$ MPa
Tensile strength	1071 MPa	632 MPa
Elongation	16%	24%
Reduction of area	41%	55%

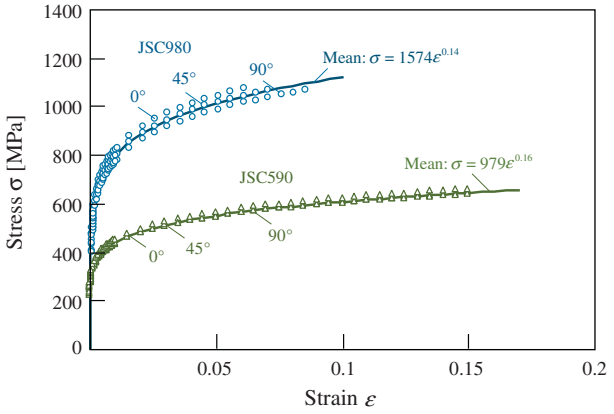

Figure 4. Flow stress curves for JSC980 and JSC590 measured from tensile test.

Table 3. Material constants for JSC980 used in calculation.

Young's modulus	210 GPa
Poisson's ratio	0.3
Initial relative density	0.995 (f_0 = 0.005)
Void nucleation parameters	ε_N = 0.3, s_N = 0.1 and f_N = 0.04
Porous failure criteria	f_F = 0.25 and f_c = 0.15

elastic-plastic and isotropic, whereas the die, sheet holder and punch were assumed to be rigid. The sheet was divided into 4-node quadrilateral ring elements. The coefficient of friction at the interfaces between the tools and sheet was assumed to be 0.1. ALE adaptive remeshing was employed to simulate severe plastic deformation in the punching process, and the Gurson damage model developed by Tvergaard [19] was included to simulate fracture in punching.

Gurson's yield criterion is defined as the following function of a void volume fraction f:

$$\Phi = \left(\frac{\bar{\sigma}}{\sigma_y}\right)^2 + 2q_1 f \cosh\left(q_2 \frac{3\sigma_m}{2\sigma_y}\right) - \left(1 - q_3 f^2\right) = 0,$$

where $\bar{\sigma}$ is the equivalent stress, σ_y is the tensile yield stress and σ_m is the hydrostatic stress. Tvergaard (1991) determined the values of the material parameters, q_1 = 1.5, q_2 = 1 and $q_3 = q_1^2 = 2.25$.

The total change in the void volume fraction is given as:

$$\dot{f} = \dot{f}_{\mathrm{gr}} + \dot{f}_{\mathrm{nucl}},$$

where $\dot{f}_{\mathrm{gr}}$ is the change due to growth of existing voids and $\dot{f}_{\mathrm{nucl}}$ is the change due to nucleation of new voids given by the strain-controlled relationship:

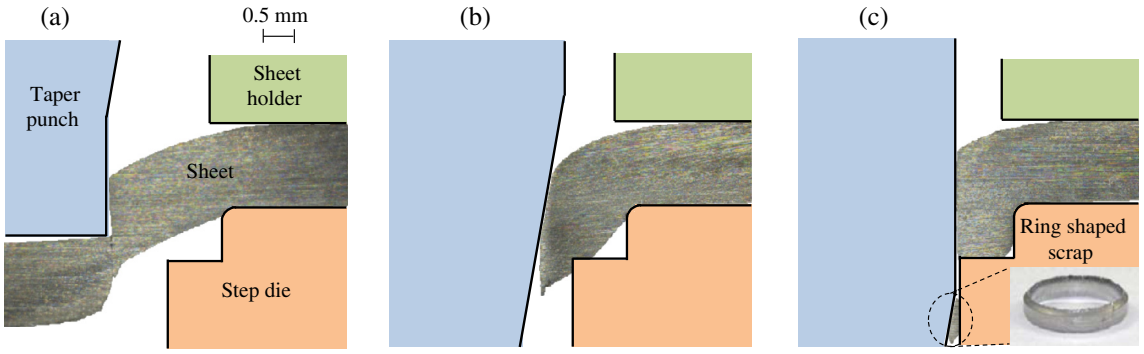

Figure 5. Deformation behaviour of sheet during punching obtained from experiment for $\theta = 10°$, $h = 0.9$ mm, JSC980 and (a) $s = 2$ mm, (b) $s = 7$ mm and (c) $s = 10$ mm.

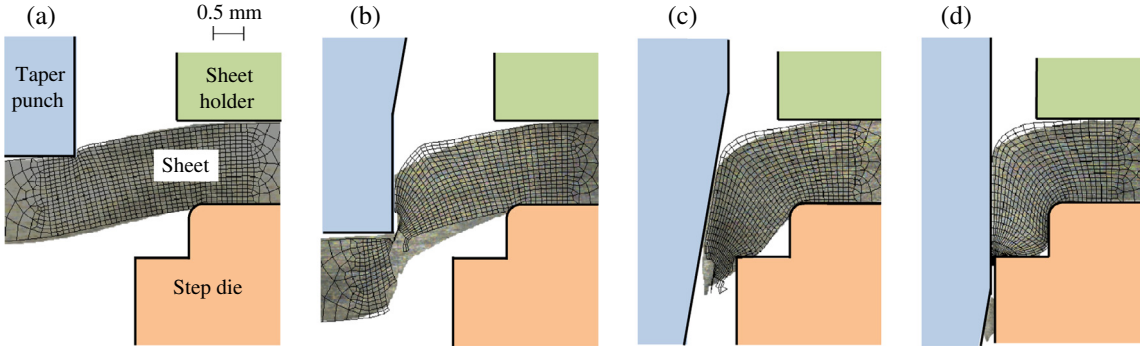

Figure 6. Comparison between deformation behaviours obtained from calculation and experiment for $\theta = 10°$, $h = 0.9$ mm, JSC980 and (a) $s = 0.55$ mm, (b) $s = 2$ mm, (c) $s = 7$ mm and (d) $s = 10$ mm.

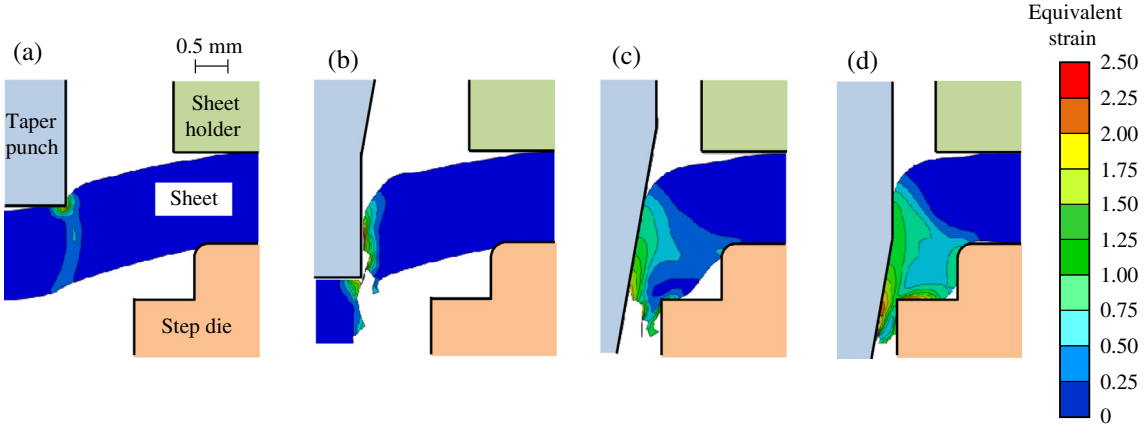

Figure 7. Distribution of plastic equivalent strain in sheet calculated by finite element simulation for $\theta = 10°$, $h = 0.9$ mm, JSC980 and (a) $s = 0.85$ mm, (b) $s = 2$ mm, (c) $s = 7$ mm and (d) $s = 9$ mm.

$$\dot{f}_{\text{nucl}} = A\dot{\bar{\varepsilon}}_m^{pl},$$

where

$$A = \frac{f_N}{s_N\sqrt{2\pi}} \exp\left[-\frac{1}{2}\left(\frac{\dot{\bar{\varepsilon}}_m^{pl} - \varepsilon_N}{s_N}\right)^2\right],$$

where ε_N is the mean value for void nucleation, s_N is the standard deviation and f_N is the volume fraction of the nucleated voids.

The material constants for JSC980 used in the calculation are shown in Table 3. The input parameters for the damage model were determined by equalising the calculated shape of

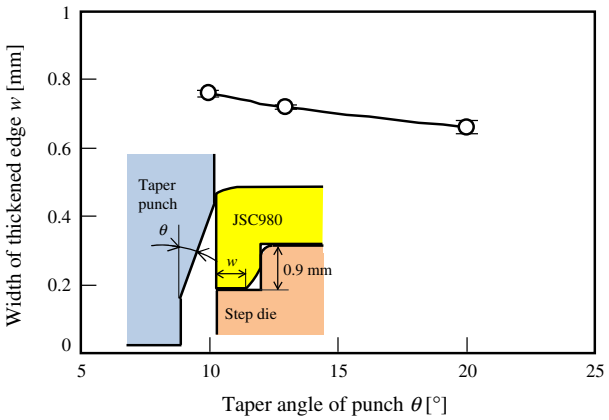

Figure 8. Relationship between width of thickened edge and taper angle of punch obtained from experiment for $h = 0.9$ mm and JSC980.

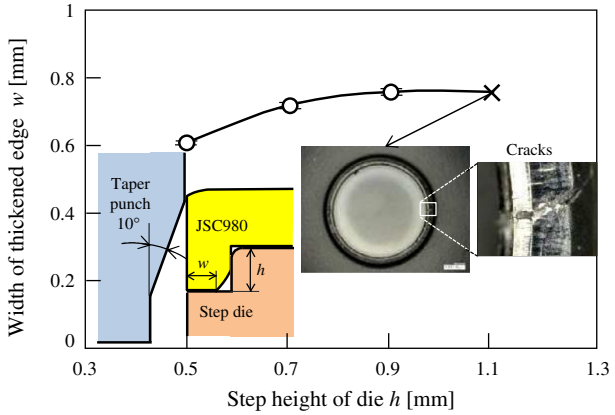

Figure 9. Relationship between width of thickened edge and step height of die obtained from experiment for $\theta = 10°$ and JSC980.

the sheared surface with that for the experimental result in the simulation of the punching process using a flat punch.

3 Results of punching including thickening of hole edge

3.1 Deformed shape

The deformation behaviour of the sheet during punching obtained from the experiment for the taper angle of the punch $\theta = 10°$, the step height of the die $h = 0.9$ mm and JSC980 is shown in Figure 5, where s is the punch stroke. The sheet is bent and punched in the former stage by the bottom of the punch, and then the hole edge is thickened by the taper of the punch and the corner step of the die. Since the material is sufficiently filled into the corner step, a ring shaped scrap is caused.

The deformation behaviour during punching was calculated from the finite element simulation in detail. A comparison between the deformation behaviours obtained from the calculation and experiment for $\theta = 10°$, $h = 0.9$ mm and JSC980 is shown in Figure 6, where the calculation results is shown as a top layer on the cross section of the experiment results. The deformation behaviour of the sheet during punching obtained by the calculation is in almost good agreement with that by the experiment, whereas the experimental rollover is more remarkable.

The distribution of plastic equivalent strain in the sheet calculated by the finite element simulation for $\theta = 10°$, $h = 0.9$ mm and JSC980 is shown in Figure 7. As the punch stroke increases, the equivalent strain concentrates around the bottom corner of the punch, and the sheet is punched. The sheared edge undergoes severe deformation with the taper and upper corner of the punch.

The relationship between the width of the thickened edge and the taper angle of the punch obtained from the experiment for $h = 0.9$ mm and JSC980 is shown in Figure 8. As the taper angle of the punch decreases, the width of the thickened edge increases, whereas the taper angle was limited to $\theta = 10°$ due the increase in stroke required for punching. For the small taper angle, the material flow in the circumferential direction is accelerated, and thus the material filling into the corner step of the die increases. The width of the thickened edge for $\theta = 10°$ is the largest, and thus $\theta = 10°$ was fixed in the following experiments.

The relationship between the width of the thickened edge and the step height of the die obtained from the experiment for $\theta = 10°$ and JSC980 is shown in Figure 9. As the step height of the die increases, the width of the thickened edge increases. When the step height of the die is small, the sheared edge is not sufficiently flanged because of early contact with the step of the die. For $h = 1.1$ mm, cracks occurred at the bottom of the thickened edge because of late contact with the die step.

The distributions of void volume fraction in the sheet calculated by the finite element simulation for $\theta = 10°$, $s = 9$ mm, JSC980 and $h = 0.5$, 0.9 and 1.1 mm are given in Figure 10. When the void fraction exceeds a critical value, the fracture occurs in the simulation of the punching stage, and thus the void fraction is extremely high around the sheared edge. The void fraction in the bottom of the thicken edge for $h = 1.1$ mm becomes high, whereas that in the top surface is not very high. This process can be applied to a less ductile material by decreasing the step height of the die, while the amount of thickening decreases.

The forming load obtained from the experiment for $\theta = 10°$, $h = 0.9$ mm and JSC980 is compared with that without thickening using a flat punch without a taper in Figure 11, where the ratio of clearance between the punch and die to the sheet thickness for the flat punch was 20%. The result for the non-coated punch was added as a comparison. The forming load with thickening has two peaks. The first peak is caused by punching the sheet and is smaller than that without thickening and the second peak. The second peak is mainly generated by ironing the sheared edge and by shearing excessive material after sufficient filling into the corner step of the die. Since the forming loads with and without coating are almost similar, the frictional effect is not large. The punching stroke with thickening is much larger than that without thickening.

The maximum forming load and forming energy with and without thickening obtained from the experiment for $\theta = 10°$

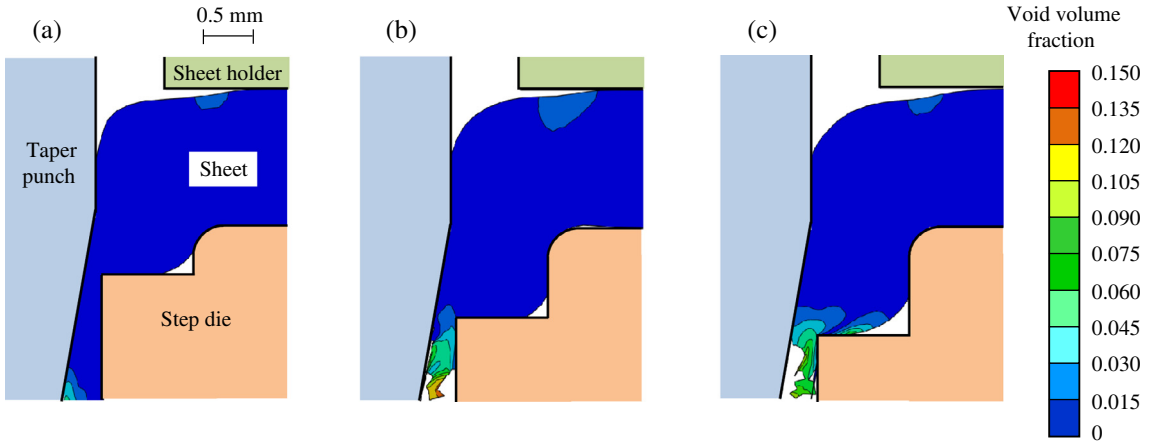

Figure 10. Distributions of void volume fraction in sheet calculated by finite element simulation for $\theta = 10°$, $s = 9$ mm, JSC980 and (a) $h = 0.5$ mm (b) $h = 0.9$ mm and (c) $h = 1.1$ mm.

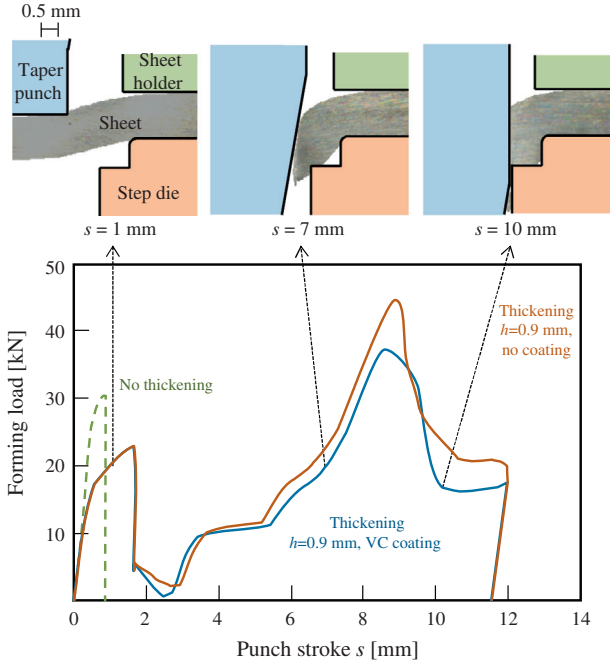

Figure 11. Forming load-punch stroke curves with thickening for $\theta = 10°$, $h = 0.9$ mm and JSC980 and without thickening obtained from experiment.

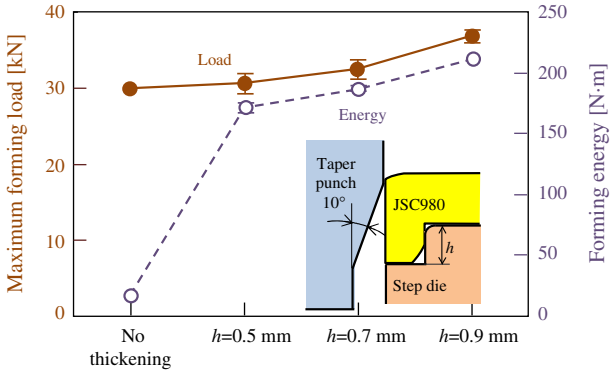

Figure 12. Maximum forming load and forming energy with and without thickening obtained from experiment for $\theta = 10°$ and JSC980.

and JSC980 are illustrated in Figure 12. The forming energy was calculated by integrating the forming load-punch stroke curve shown in Figure 11. As the step height of the die increases, the forming load and energy increase. The forming energy with thickening becomes considerably large due to the enlargement of the punch stroke.

3.2 Quality of sheared edge

The surfaces and cross-sections of the sheared edge with and without thickening obtained from the experiment for $\theta = 10°$ and JSC980 are shown in Figure 13. As the step height of the die increases, the amount of thickening increases. The area of the rough fracture surface without thickening is considerably improved by thickening. Although the depth of the rollover for thickening is larger than that without thickening due to bending during punching by the bottom of the punch, the depth is almost constant for the step height of the die. The rollover can be reduced by separating the step portion from the die and by pressing back the sheared edge portion with the separated step portion after thickening. Since this separation complicates structure of tools, the effect of thickening on the fatigue strength was evaluated without improvement of the rollover.

The distributions of the arithmetic mean value of the surface roughness of the sheared edge in the thickness direction with and without thickening obtained from the experiment for $\theta = 10°$, $h = 0.9$ mm and JSC980 are shown in Figure 14. The surface roughness was measured at intervals of 0.1 mm in the thickness direction. The surface roughness of the thickened sheared edge is considerably smaller than that without thickening due to the elimination of fracture surface. Although the surface roughness without thickening scatters, the scatter with thickening is very small.

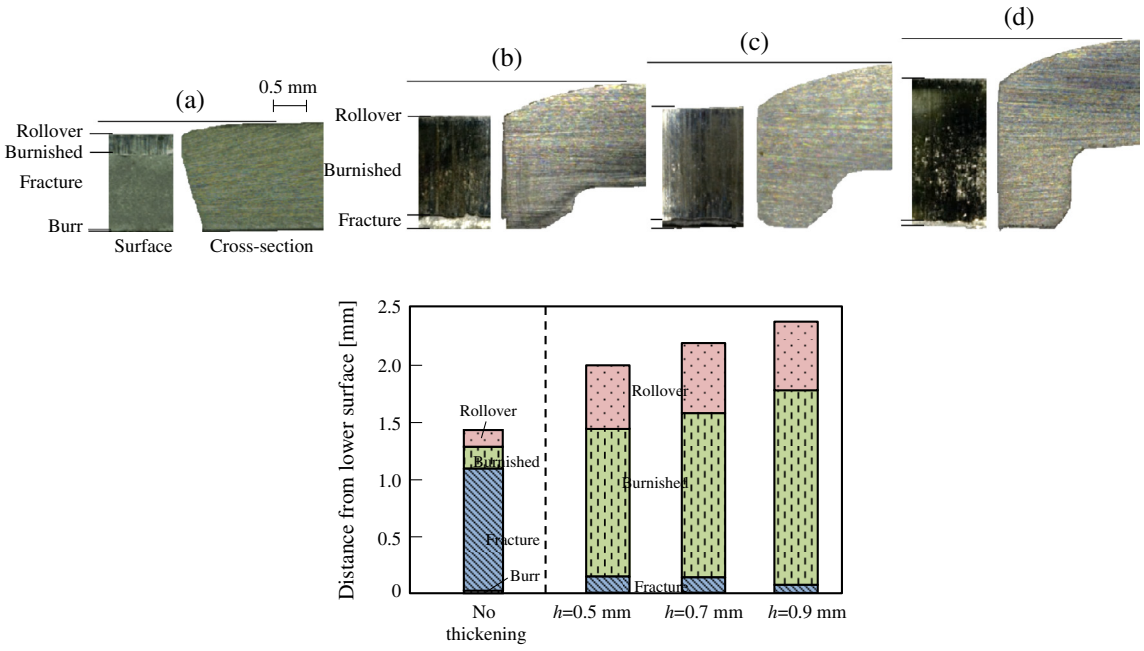

Figure 13. Surface and cross-section of sheared edge obtained from experiment for θ = 10°, JSC980, (a) no thickening, (b) h = 0.5 mm, (c) h = 0.7 mm and (d) h = 0.9 mm.

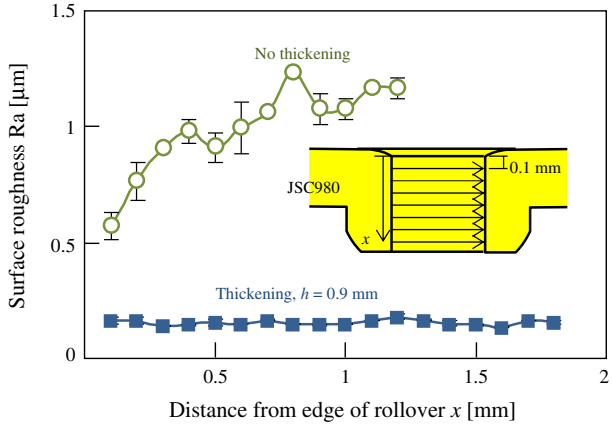

Figure 14. Distributions of arithmetic mean value of surface roughness of sheared edge in thickness direction with and without thickening obtained from experiment for θ = 10°, h = 0.9 mm and JSC980.

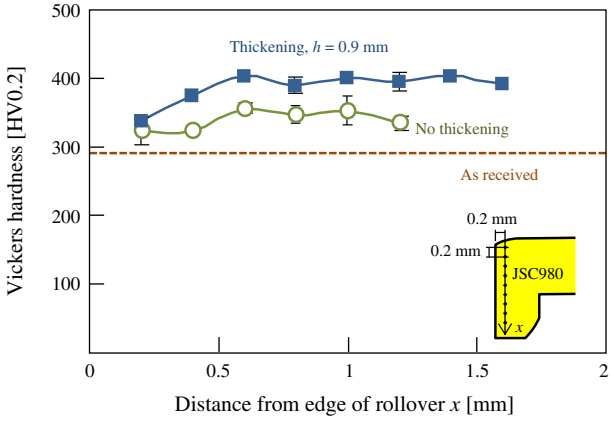

Figure 15. Distributions of Vickers hardness in thickness direction around sheared edge with and without thickening obtained from experiment for θ = 10°, h = 0.9 mm and JSC980.

The distributions of Vickers hardness in the thickness direction around the sheared edge with and without thickening obtained from the experiment for θ = 10°, h = 0.9 mm and JSC980 are shown in Figure 15. The hardness was measured in the cross-section at 0.2 mm from the sheared edge with intervals of 0.2 mm in the thickness direction. The hardness with thickening is higher than that without thickening due to ironing with the taper of the punch.

To examine the work-hardening behaviour around the sheared edge due to the punching and thickening, the distributions of Vickers hardness was measured for different distances from the sheared edge y, θ = 10°, h = 0.9 mm and JSC980 as shown in Figure 16. The hardness was measured in the cross-section at 0.2, 0.4 and 0.6 mm from the sheared edge at intervals of 0.2 mm in the thickness direction. As the distance from the sheared edge increases, the hardness decreases. The hardness near the sheared edge was the largest due to the influence of ironing with the taper of the punch.

The residual stress in the sheared edge of the punched sheet was measured by the X-ray diffraction. A diffraction angle 2θ of the X-ray was set between 153.0° and 157.8° at intervals of 0.02°. The residual stress on the surface of the sheared edge for ψ = 90° was obtained by extrapolating the stress obtained

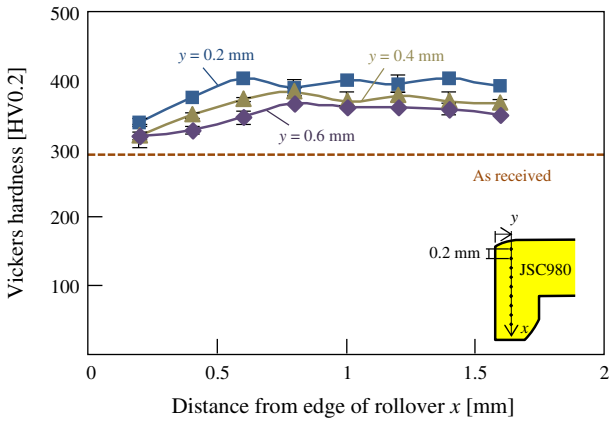

Figure 16. Distributions of Vickers hardness in thickness direction around sheared edge obtained from experiment for different distance from sheared edge y, θ = 10°, h = 0.9 mm and JSC980.

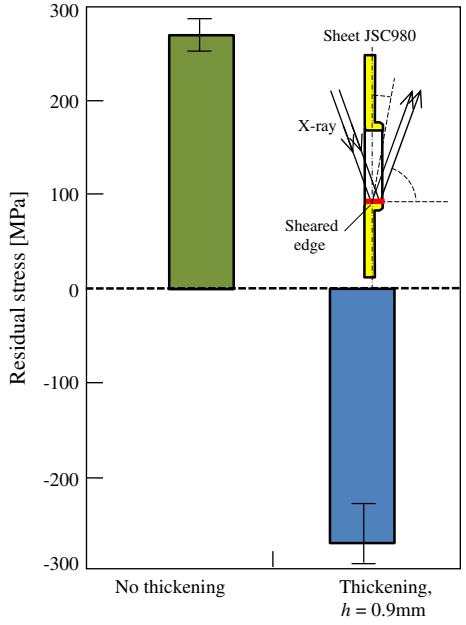

Figure 17. Residual stresses in thickness direction in sheared edge of punched sheets with and without thickening measured by X-ray diffraction for θ = 10°, h = 0.9 mm and JSC980.

for inclination angles ψ of 0°, 18°, 27°, 33° and 45°. The residual stresses in the thickness direction in the sheared edge of the punched sheets with and without thickening for θ = 10°, h = 0.9 mm and JSC980 are shown in Figure 17. Although the residual stress without thickening is tensile, the stress with thickening becomes compressive due to the ironing during the thickening stage.

4 Strength of punched sheet

4.1 Fatigue strength

The bending and tensile fatigue tests of the punched sheets with the thickened hole edge were performed. The procedure and dimensions of specimens for the two fatigue tests are shown in Figure 18. The fatigue test was performed each condition at least two times and the averages of the measured values are shown. The frequencies for the alternative bending and repeated tensile fatigue tests were set at 25 and 50 Hz, respectively. The fatigue test was ended when the sheet was ruptured. The maximum number of cycles for the fatigue tests was 10^7. Since the stress is complexly distributed in the punched sheet during the fatigue tests due to stress concentration around the punched holes, the nominal stress calculated for a sheet without a hole and thickening is indicated in the following results. For bending, the maximum bending stress calculated on the surface of the sheet is indicated.

The plots of the nominal stress amplitude versus the number of cycles to failure for θ = 10°, the bending and tensile fatigue tests of the punched sheets with thickening are compared with those without thickening in Figure 19, where no rupture occurred for the numbers of cycles of 10^7. As the step height of the die increases, the fatigue strength increases. The fatigue strength of the punched sheets with thickening is considerably higher than that without thickening. The increase in fatigue strength with thickening for JSC980 was larger than that for JSC590. The improvement of the fatigue strength for thickening is due to the decrease in stress by the thickening, the compressive stress, the small surface roughness and the large hardness around the sheared edge. It was found that thickening of the hole edge is useful for improving the fatigue strength of punched ultra-high strength steel sheet.

4.2 Delayed fracture

Mori et al. [10] reported that punched ultra-high strength steel sheet have the risk of delayed fracture. The occurrence of delayed fracture on the sheared edge was visually observed by keeping the punched sheets in 35% concentration hydrochloric acid at room temperature. The occurrence of delayed fracture was accelerated with the high concentration of the acid.

The effect of thickening of the hole edge on the occurrence of the delayed fracture time obtained from the experiment for θ = 10°, h = 0.9 mm and JSC980 is given in Figure 20, where the delayed fracture time is the time from the soak of the sheet in the acid. Although cracks were observed after 2.5 h for the punched sheet without thickening, no cracks were observed up to 48 h for the thickened sheet. For no thickening, the rough fracture surface in the sheared edge containing microcracks becomes large, and thus the hydrogen tends to diffuse. Moreover, the tensile residual stress in the sheared edge accelerates the occurrence of the delayed fracture. The delayed fracture for the thickening was prevented due to the large compressive stress and the small surface roughness.

4.3 Static strength

To investigate the effect of the thickening on the static strength of the punched sheets, the static tensile test was carried out. The procedure and dimensions of specimen for the static test were the same with those for the fatigue tensile test shown in Figure 18b and 18c. The static test was performed each

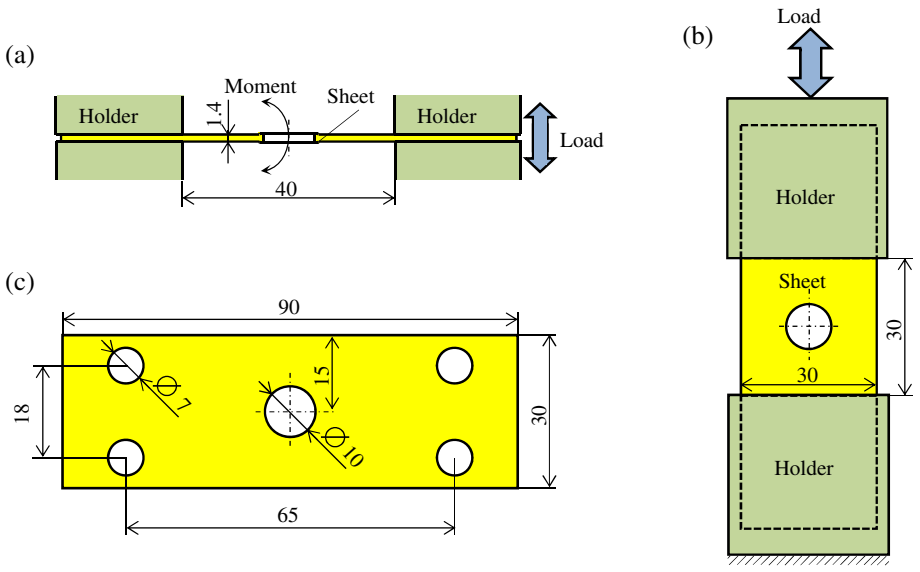

Figure 18. Procedure of (a) bending and (b) tensile fatigue tests and (c) dimensions of specimens.

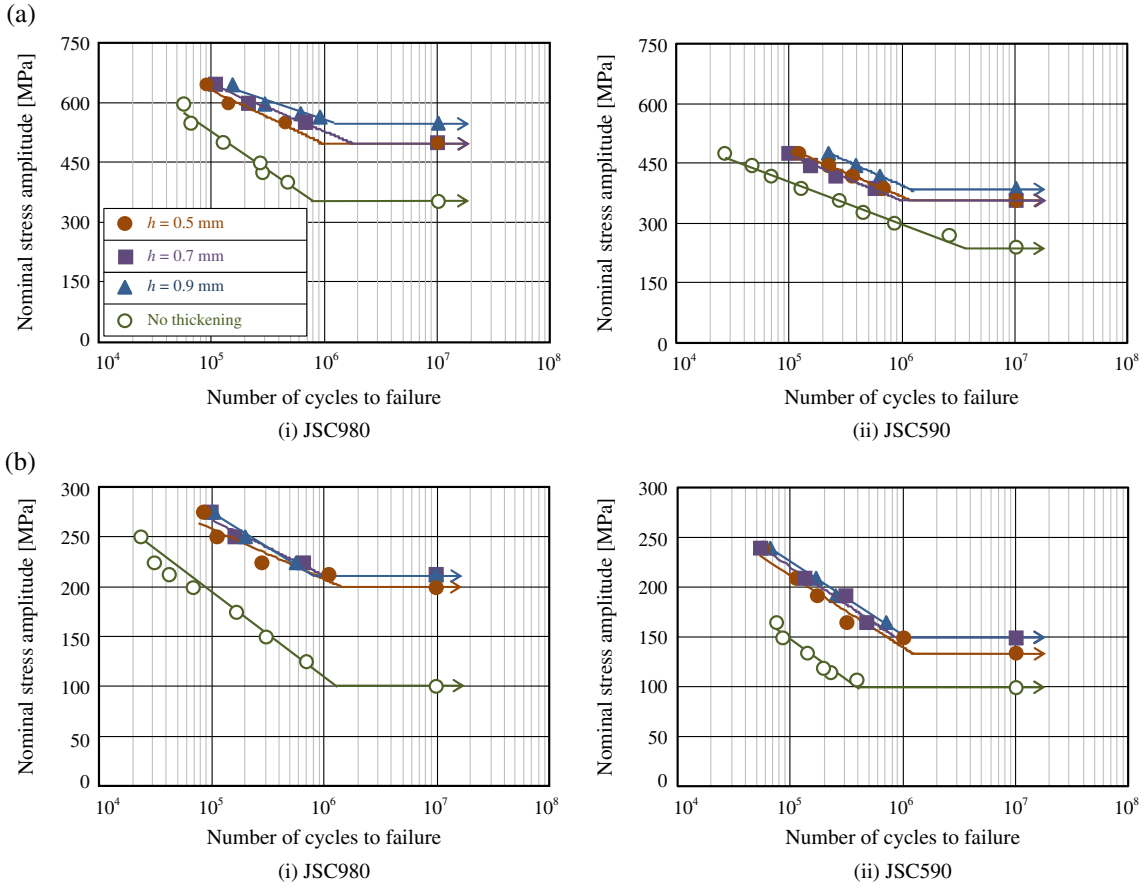

Figure 19. Plots of nominal stress amplitude versus number of cycles to failure of punched sheets with and without thickening for $\theta = 10°$, (a) bending and (b) tensile fatigue tests.

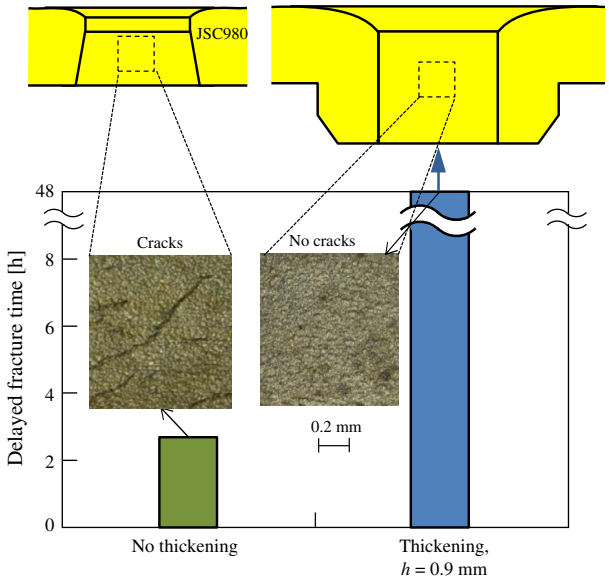

Figure 20. Effect of thickening of hole edge on occurrence of delayed fracture time obtained from experiment for $\theta = 10°$, $h = 0.9$ mm and JSC980.

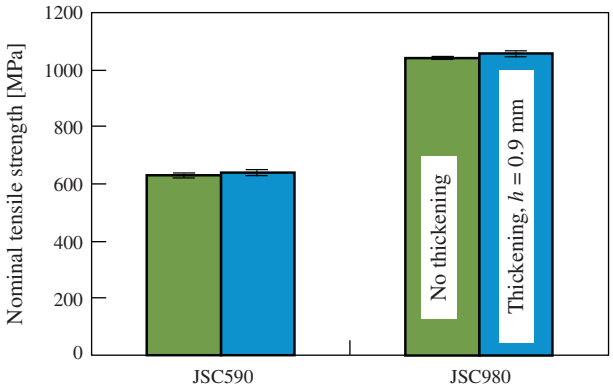

Figure 21. Nominal tensile strength of punched sheets with and without thickening obtained from experiment for $\theta = 10°$, $h = 0.9$ mm.

condition at least two times and the averages of the measured values are shown.

The nominal tensile strength of the punched sheets with and without thickening obtained from the experiment for $\theta = 10°$, $h = 0.9$ mm is shown in Figure 21. The increase in the static strength for the thickening for both JSC590 and JSC980 was comparatively small due to the small increase in area, only 5% increase.

5 Repeated punching including thickening of hole edge

Since the above mentioned results were obtained for a slow punching speed of 0.08 mm/s, repeated punching was carried out under a realistic punching speed of 100 mm/s to check the applicability of the present punching process to actual stamping operations. The ultra-high strength steel sheet JSC980 was punched for $\theta = 10°$ and $h = 0.9$ mm with a CNC servo press having a capacity of 800 kN. The punch was VC-coated by Toyota diffusion coating process and the hardness was 3500 HV. The wear and seizure resistances of this coating are very high and thus the required amount of lubricant could be reduced.

The surface and cross-section of the sheared edge in repeated punching for $\theta = 10°$, $h = 0.9$ mm and JSC980 are shown in Figure 22, where n is the number of strikes. The surface quality of the sheared edge is high and the geometry of the cross section is hardly changed even for $n = 100$.

The surface of the punch in repeated punching for $\theta = 10°$, $h = 0.9$ mm and JSC980 is given in Figure 23. The surface of the VC-coated punch hardly changed even for $n = 100$,

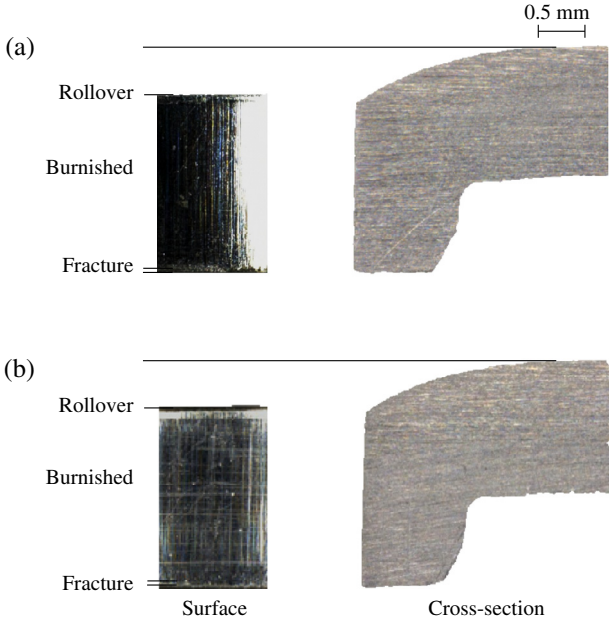

Figure 22. Surface and cross-section of sheared edge in repeated punching for $\theta = 10°$, $h = 0.9$ mm, JSC980, (a) $n = 1$ and (b) $n = 100$.

whereas seizure occurred due to severe shear deformation for the non-coated punch and $n = 1$.

6 Conclusions

A punching process including thickening of a hole edge of ultra-high strength steel sheet was developed to improve fatigue strength of the punched sheet. A pair of taper punch and step die was designed to include thickening of the hole edge in the punching process and easily installed in conventional die sets. A part of the punching scrap was effectively utilised as

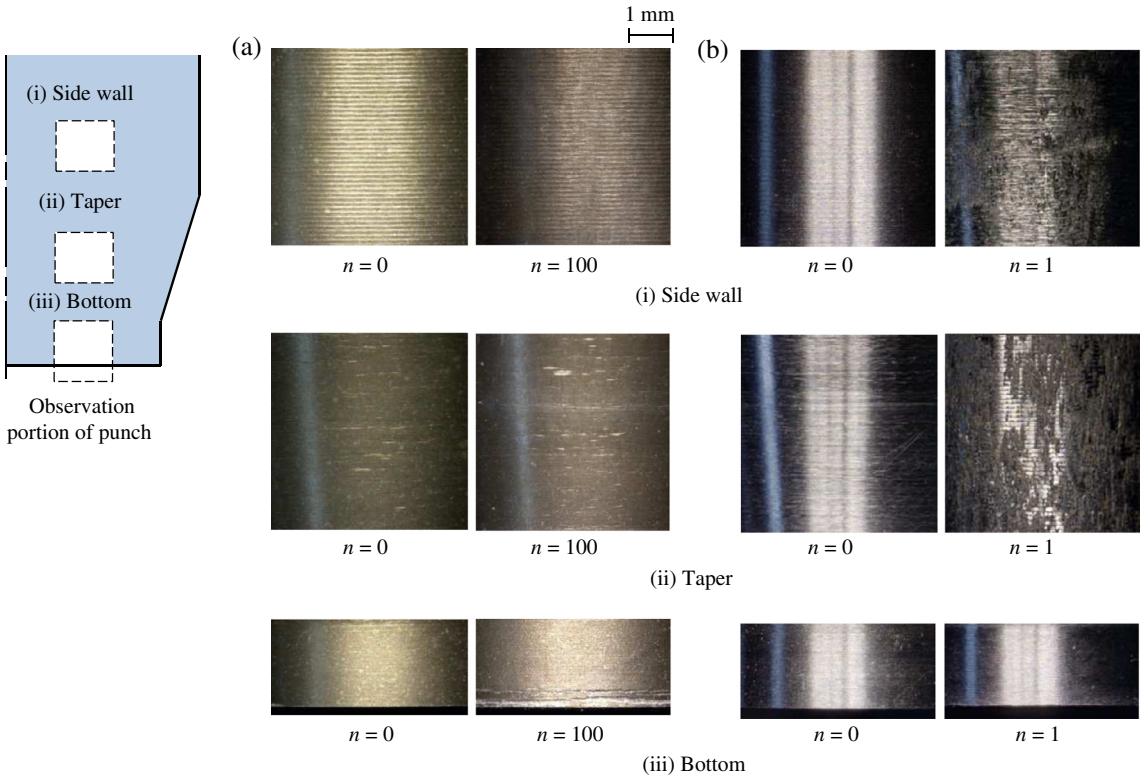

Figure 23. Surface of punch in repeated punching for $\theta = 10°$, $h = 0.9$ mm, JSC980, punches (a) with and (b) without VC coating.

thickening materials in the present process. This is an ecological process for improving material efficiency. The results are summarised as follows:

1. The sheet was punched in the former stage by the bottom of the punch, and then the hole edge was thickened by the taper of the punch and the corner step of the die.
2. The surface quality of the sheared edge with thickening was improved due to ironing with the taper of the punch during the thickening stage.
3. The fatigue strength of the punched sheets with thickening was considerably higher than that without thickening due to the decrease in stress by the thickening, the compressive stress, the small surface roughness and the large hardness around the sheared edge.
4. The delayed fracture was prevented by thickening due to the large compressive residual stress and the small surface roughness.

Implications and influences

The use of the ultra-high strength steel sheets for automobile parts is increasing, whereas the applicable range is still limited to the fatigue strength. For example, the ultra-high strength steel sheets are not applied to automobile wheels subjected to cyclic loading due to insufficient fatigue strength. The fatigue strength of the ultra-high strength steel sheets is not increased as much as the static strength. Although microstructure in the ultra-high strength steel sheets is controlled in steel making industry to heighten the fatigue strength, forming of products having high fatigue strength is an alternative approach. The fatigue strength can be increased by relieving concentration of tensile stress during loading, particularly relieving around sheared edges such as the present process is considerably effective. Since the thicken hole edges becomes projections, this side is required to be designed inside parts.

References

1. M. Kleiner, M. Geiger, A. Klaus, Bulk sheet metal forming, CIRP Annals – Manufacturing Technology 52 (2003) 725–745.
2. K. Mori, K. Akita, Y. Abe, Springback behaviour in bending of ultra-high-strength steel sheets using CNC servo press, International Journal of Machine Tools and Manufacture 47 (2007) 321–325.
3. J. Eriksson, M. Olssson, Tribological testing of commercial CrN, (Ti,Al)N and CrC/C PVD coatings – Evaluation of galling and wear characteristics against different high strength steels, Surface & Coating Technology 205 (2011) 4045–4051.
4. K. Inoue, M. Suzuki, S. Nishino, K. Ohya, Y. Tomota, Effect of coating microstructure of press-working dies on sliding damage, Steel Research International 81, Supplement Metal Forming 2010 (2010) 849–852.
5. Y. Murakami, S. Kodama, S. Konuma, Quantitative evaluation of effects of non-metallic inclusions on fatigue strength of high strength steels. I: Basic fatigue mechanism and evaluation of correlation between the fatigue fracture stress and the size and location of non-metallic inclusions, International Journal of Fatigue 11 (1989) 291–298.

6. D.J. Thomas, M.T. Whittaker, G. Bright, Y. Gao, The influence of mechanical and CO_2 laser cut-edge characteristics on the fatigue life performance of high strength automotive steels, Journal of Materials Processing Technology 211 (2011) 263–274.
7. S. Thipprakmas, S. Rojananan, P. Paramaputi, An investigation of step taper-shaped punch in piercing process using finite element method, Journal of Materials Processing Technology 197 (2008) 132–139.
8. S.S. Kim, C.S. Han, Y.S. Lee, Development of a new burr-free hydro mechanical punching, Journal of Materials Processing Technology 162–163 (2005) 524–529.
9. K. Mori, Y. Abe, Y. Suzui, Improvement of stretch flangeability of ultra-high strength steel sheet by smoothing of sheared edge, Journal of Materials Processing Technology 210 (2010) 653–659.
10. K. Mori, Y. Abe, Y. Kidoma, P. Kadarno, Slight clearance punching of ultra-high strength steel sheets using punch having small round edge, International Journal of Machine Tools and Manufacture 65 (2013) 41–46.
11. Y. Abe, K. Mori, K. Norita, Gradually contacting punch for improving stretch flangeability of ultra-high strength steel sheets, CIRP Annals – Manufacturing Technology 62 (2013) 263–266.
12. K. Mori, S. Saito, S. Maki, Warm and hot punching of ultra-high strength steel sheet, CIRP Annals – Manufacturing Technology 57 (2008) 321–324.
13. D.J. Thomas, Effect of mechanical cut-edges on the fatigue and formability performance of advanced high-strength steels, Journal of Failure Analysis and Prevention 12 (2012) 518–531.
14. T. Matsuno, Y. Kuriyama, H. Murakami, S. Yonezawa, H. Kanamaru, Effects of punch shape and clearance on hole expansion ratio and fatigue properties in punching of high strength steel sheets, Steel Research International 81, Supplement Metal Forming 2010 (2010) 853–856.
15. T. Nakano, Introduction of Flow Control Forming (FCF) for sheet forging and new presses, in Proceedings of the International Seminar on Precision Forging, Kyoto, 1973, p. 35–40.
16. M. Merklein, J.M. Allwood, B.-A. Behrens, A. Brosius, H. Hagenah, K. Kuzman, K. Mori, A.E. Tekkaya, A. Weckenmann, Bulk sheet metal forming, CIRP Annals – Manufacturing Technology 61 (2012) 725–745.
17. P. Kadarno, K. Mori, Y. Abe, Two-stage plate forging for thickening hole edge of punched high strength steel sheet, in Proceedings of 14th International Conference on Metal Forming, Krakow, 2012, p. 899–902.
18. S. Thipprakmas, M. Jin, M. Murakawa, Study on flanged shapes in fineblanked-hole flanging process (FB-hole flanging process) using finite element method (FEM), Journal of Materials Processing Technology 192–193 (2007) 128–133.
19. V. Tvergaard, Mechanical modelling of ductile fracture, Meccanica 26 (1991) 11–16.

Cite this article as: Kadarno P, Mori K-I, Abe Y & Abe T: Punching process including thickening of hole edge for improvement of fatigue strength of ultra-high strength steel sheet. Manufacturing Rev. 2014, **1**, 4.